

Electronic Supplementary Information

3D Porous Hierarchical $\text{Li}_2\text{FeSiO}_4/\text{C}$ for Rechargeable Lithium Batteries

Ling Zhang,^a Jiangfeng Ni,^{*a} Wencong Wang,^a Jun Guo^b and Liang Li^{*a}

^aCollege of Physics, Optoelectronics and Energy, Soochow University, Suzhou 215006, China

^bTesting and Analysis Center, Soochow University, Suzhou 215123, China

*Corresponding authors. Tel/Fax: +81-512-67875503

E-mail addresses: jeffni@suda.edu.cn (J. Ni), lli@suda.edu.cn (L. Li).

Materials characterization

Crystallographic information of the samples was identified by X-ray diffraction (XRD) using a Rigaku Dmax-2400 automatic diffractometer ($\text{Cu } K\alpha$). Material shape and morphology were observed by scanning electron microscopy (SEM, Hitachi S-4800) and transmission electron microscopy (TEM, FEI Tecnai G2 T20). Raman spectroscopy measurements were conducted on a JY HR800 spectrometer using an excited HeNe laser (633 nm). Thermogravimetric (TG) analysis was performed on a TG/DTA-7300 thermal analyzer (Seko). Nitrogen adsorption and desorption isotherms were measured on a Tristar 3020 micropore analyzer (Micromeritics).

Electrochemical evaluation

Electrochemical tests were performed on a 2032-type coin cell. The working electrodes were composed of 80 wt% active material, 10 wt% acetylene black, and 10 wt% polyvinylidene fluoride binder. The mass loading for the composite electrode is 2.0–2.5 mg cm^{-2} . Li foil was used as the counter electrode and GFA glass fiber filters (Whatman) as separator. The electrolyte is 1 mol l^{-1} LiPF_6 solution dissolved in ethylene carbonate/dimethyl carbonate (1:1 by volume). Cyclic voltammetry and electrochemical impedance spectroscopy were conducted on a CHI 660E electrochemical workstation. Galvanostatic tests were carried out on a Land battery test system.

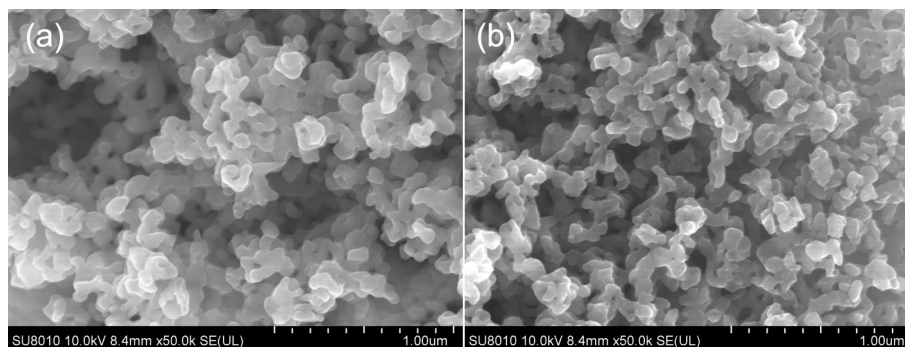


Figure S1. SEM images of 3D porous hierarchical $\text{Li}_2\text{FeSiO}_4/\text{C}$.

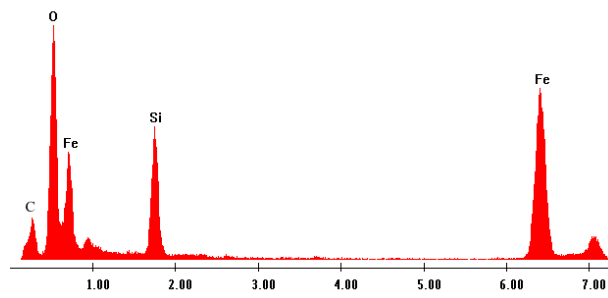


Figure S2. Energy dispersive X-ray spectroscopy of 3D porous $\text{Li}_2\text{FeSiO}_4/\text{C}$.

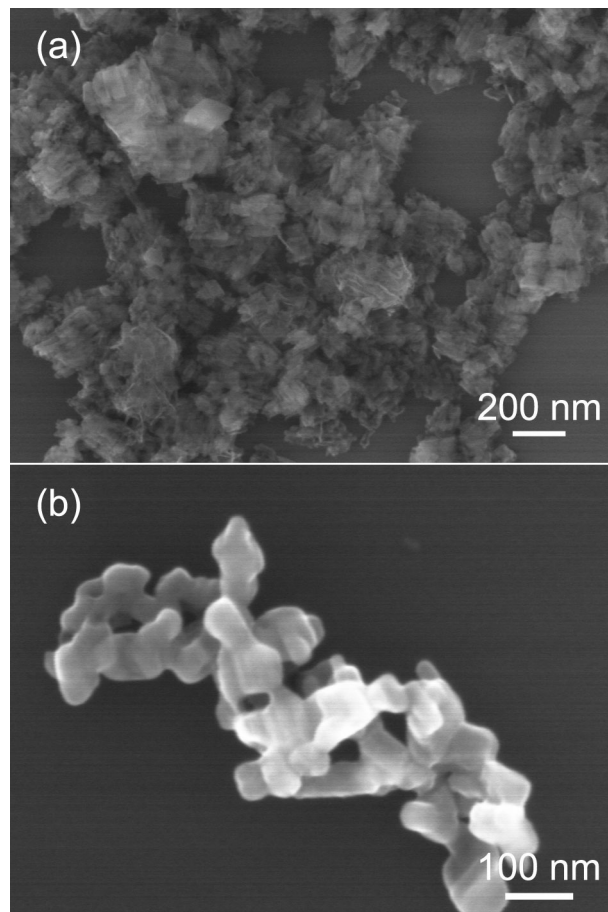


Figure S3. SEM images of (a) hydrothermal intermediate and (b) 3D $\text{Li}_2\text{FeSiO}_4$.

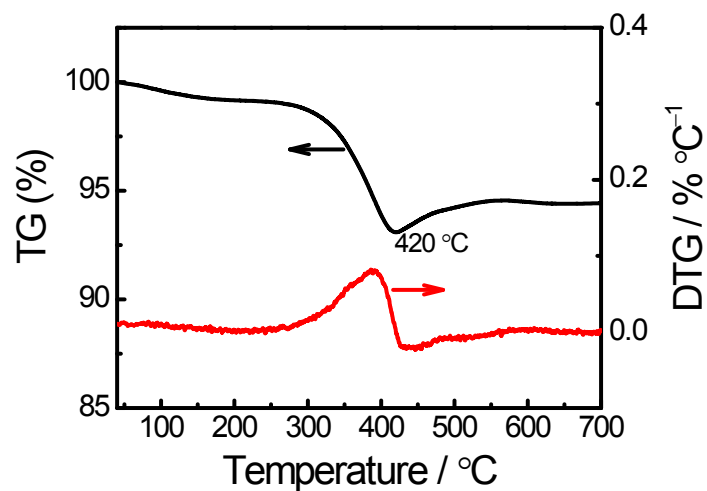


Figure S4. TG and DTG curves of 3D porous $\text{Li}_2\text{FeSiO}_4/\text{C}$.

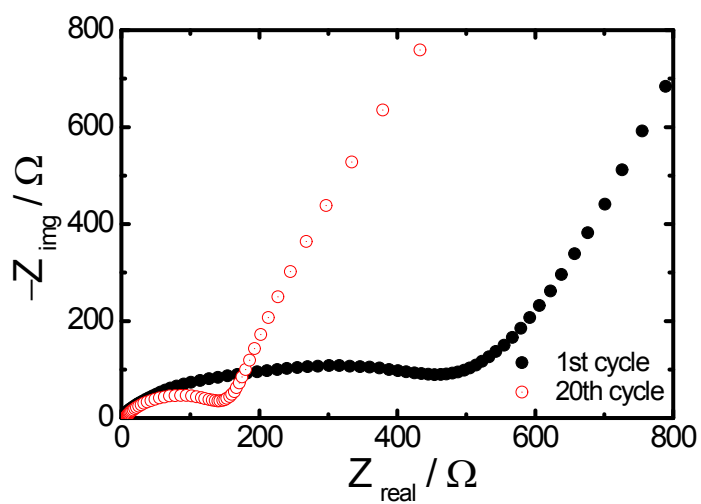


Figure S5. Nyquist plots of the impedance spectra of the 3D porous $\text{Li}_2\text{FeSiO}_4/\text{C}$ after one and 20 cycles.

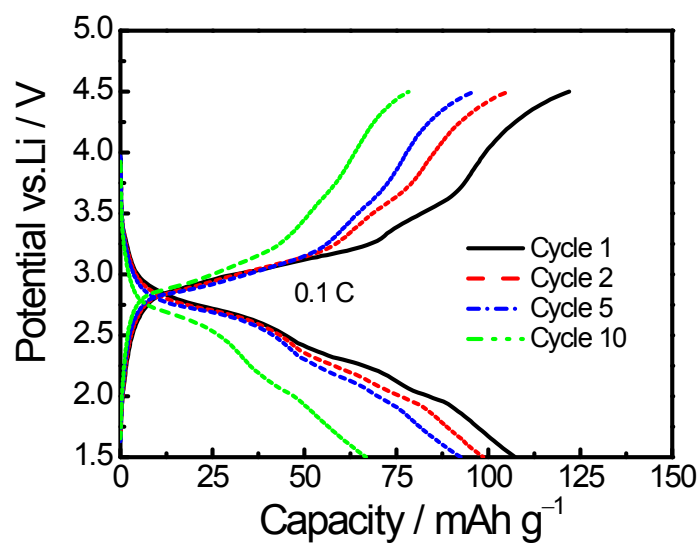


Figure S6. Typical galvanostatic curves of 3D porous $\text{Li}_2\text{FeSiO}_4$ after activation.

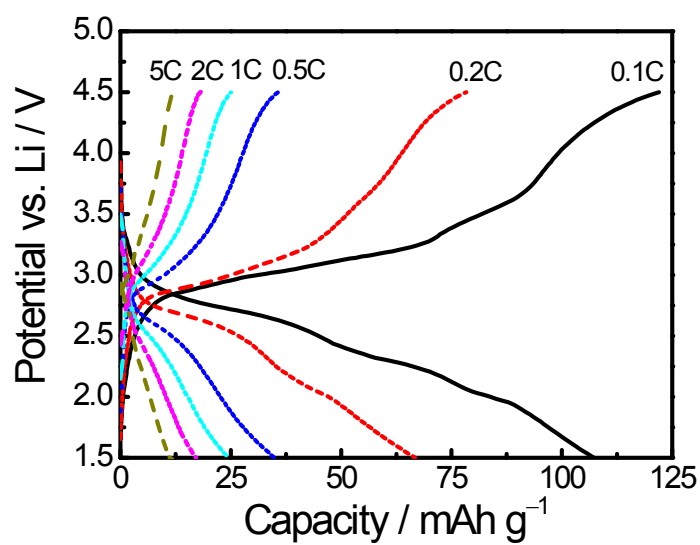


Figure S7. Rate capability of 3D porous $\text{Li}_2\text{FeSiO}_4$.